RESEARCH REPORT

126

Climate Change Impacts on Hydrology and Water Resources of the Upper Blue Nile River Basin, Ethiopia

Ungtae Kim, Jagath J. Kaluarachchi and Vladimir U. Smakhtin

International Water Management Institute

UtahState UNIVERSITY

FUTURE HARVEST
IWMI is a Future Harvest Center supported by the CGIAR

Research Reports

IWMI's mission is to improve the management of land and water resources for food, livelihoods and environment. In serving this mission, IWMI concentrates on the integration of policies, technologies and management systems to achieve workable solutions to real problems—practical, relevant results in the field of irrigation and water and land resources.

The publications in this series cover a wide range of subjects—from computer modeling to experience with water user associations—and vary in content from directly applicable research to more basic studies, on which applied work ultimately depends. Some research reports are narrowly focused, analytical and detailed empirical studies; others are wide-ranging and synthetic overviews of generic problems.

Although most of the reports are published by IWMI staff and their collaborators, we welcome contributions from others. Each report is reviewed internally by IWMI's own staff and Fellows, and by external reviewers. The reports are published and distributed both in hard copy and electronically (www.iwmi.org) and where possible all data and analyses will be available as separate downloadable files. Reports may be copied freely and cited with due acknowledgment.

Research Report 126

Climate Change Impacts on Hydrology and Water Resources of the Upper Blue Nile River Basin, Ethiopia

Ungtae Kim, Jagath J. Kaluarachchi and Vladimir U. Smakhtin

International Water Management Institute
P O Box 2075, Colombo, Sri Lanka

IWMI receives its principal funding from 58 governments, private foundations, and international and regional organizations known as the Consultative Group on International Agricultural Research (CGIAR). Support is also given by the Governments of Ghana, Pakistan, South Africa, Sri Lanka and Thailand.

The authors: Dr. Ungtae Kim, formerly a PhD student of Utah State University, is currently a Postdoctoral Research Associate at the Institute for a Secure and Sustainable Environment, and a Research Assistant Professor of Civil and Environmental Engineering, University of Tennessee, Knoxville, Tennessee. Dr. Jagath J. Kaluarachchi is Associate Dean of the College of Engineering and Professor of the Department of Civil and Environmental Engineering of Utah State University. Dr. Vladimir U. Smakhtin is a Principal Scientist in Hydrology and Water Resources at the International Water Management Institute, Colombo, Sri Lanka.

Acknowledgements: This report is a summary of Dr. Ungtae Kim's PhD dissertation from Department of Civil and Environmental Engineering, Utah State University, Logan, Utah. This study was supported by a PhD Fellowship from the Inland Northwest Research Alliance (INRA) of the US Department of Energy and with travel funding from the International Water Management Institute (IWMI), Colombo, Sri Lanka. The authors would like to acknowledge the valuable insight of Drs. Yasir A. Mohamed and Seleshi B. Awulachew of IWMI. The Ministry of Water Resources of Ethiopia is also acknowledged for their help in obtaining some of the hydrologic data and GIS maps.

Kim, U.; Kaluarachchi, J. J.; Smakhtin, V. U. 2008. *Climate change impacts on hydrology and water resources of the Upper Blue Nile River Basin, Ethiopia.* Colombo, Sri Lanka: International Water Management Institute. 27p (IWMI Research Report 126)

/ climate change / hydrology / river basins / models / runoff / dams / operating policies / drought / water power / Ethiopia / Egypt / Sudan /

ISSN 1026-0862
ISBN 978-92-9090-696-4

Cover photograph: The Tis Issat (Blue Nile) Waterfall, Ethiopia

Photo credit: Seleshi Bekele Awulachew, IWMI, East Africa and Nile Basin Office, Addis Ababa, Ethiopia

Please send inquiries and comments to: iwmi@cgiar.org

Contents

Summary

This report aims to evaluate the impacts of climate change on both hydrologic regimes and water resources of the Upper Blue Nile River Basin in Ethiopia where observed hydrologic data are limited. The downstream countries of the Nile River Basin are sensitive to the variability of runoff from the Ethiopian part of the basin. This report presents three steps for analyzing climate change impacts on hydrology and water resources. The first is the construction of the climate change scenarios whereby the outcomes of multiple general circulation models (GCMs) are used to perturb the baseline climate scenario representing the current precipitation and temperature patterns. The second is runoff simulation by using a simple two-tank hydrologic model due to the limited data availability and the scale of the sub-basins. The hydrologic model uses the constructed climate scenarios as input to predict runoff. The model parameters for ungauged parts of the basin are estimated by means of hydrologic regionalization. In the final step, climate change impacts on hydrology and water resources are examined using a set of indices. The impacts of potential future hydropower dam operations in the upstream parts of the Nile Basin under future climate scenarios on downstream countries are also assessed. The results suggest that (1) the climate in most of the Upper Blue Nile River Basin is likely to become wetter and warmer in the 2050s (2040-2069); (2) low flows may become higher and severe mid- to long-term droughts are likely to become less frequent throughout the entire basin; and (3) the potential future dam operations are unlikely to significantly affect the water availability to Sudan and Egypt based on predicted outflows from six GCMs and many dam operation scenarios. The results, however uncertain with existing accuracy of climate models, suggest that the region is likely to have the future potential to produce hydropower, increase flow duration, and increase water storage capacity without affecting outflows to the riparian countries in the 2050s.

Climate Change Impacts on Hydrology and Water Resources of the Upper Blue Nile River Basin, Ethiopia

Ungtae Kim, Jagath J. Kaluarachchi and Vladimir U. Smakhtin

Introduction

The impacts of climate change on water resources are high on the research agenda worldwide (IPCC 2007). Future changes in overall flow magnitude, variability and timing of the main flow events are among the most frequently cited hydrologic issues (Frederick 2002; Wurbs et al. 2005). These changes may have a high impact on transboundary river basins where competition for water is from stakeholders from different economic, political and social backgrounds while changing runoff variability of upstream countries can affect the downstream countries. A typical example is the Nile River Basin which consists of the White Nile and the Blue Nile. Most parts of the Nile Basin are found to be sensitive to climatic variations (Conway and Hulme 1996; Yates and Strzepek 1998a,b; Conway 2005). The Blue Nile which constitutes only around 10% of the entire Nile Basin area, however, contributes about 60% of its total mean annual flow measured at the *High Aswan Dam* (Waterbury 1979; Sutcliffe and Parks 1999; Conway 2005). Thus, runoff variability in upstream countries, such as Ethiopia where most of the Blue Nile flow is generated, is of great importance to the sustainable development of downstream countries such as Sudan and Egypt where most of the Nile water is used in accordance with the 1959 water sharing agreement (Yates and Strzepek 1998a; Tafesse 2001; Conway 2005). The increasing water demand of upstream countries in the Nile Basin coupled with climate change impacts can affect the availability of water resources for downstream countries and in the basin.

Previous studies which examined the impacts of climate change on water resources in the Nile Basin (Gleick 1991; Conway and Hulme 1993,1996; Strzepek and Yates 1996; Yates and Strzepek 1996,1998a,b; Sene et al. 2001; Conway 2005), have mostly focused on the changes in runoff and their consequences for the economies of downstream countries. However, climate change can affect multiple features of water resources, e.g., quantity and quality, high- and low-flow extremes, timing of events, water temperature, etc. All these aspects affect livelihoods in the basin but have not received attention in planning for future water allocation and design of water infrastructure yet.

Since 1999, a multilateral effort called the Nile Basin Initiative has been underway to promote the cooperation to maximize the benefits of Nile water (Whittington et al. 2005). Ethiopia, for example, can be endowed with economic benefits due to the tremendous potential for hydropower generation and irrigation associated with the country's advantageous geographical location in the Nile Basin. In 1964, the US Bureau of Reclamation (USBR 1964) identified four hydropower sites, *Karadobi*, *Mabil*, *Mendaia* and *Border*, in the main stem of the study area (Figure 1). More recently, Block (2007) assessed the benefit-cost ratios of these potential future USBR dams under operational policies, water abstractions, and climate change scenarios. Although several studies identifying the feasibility of hydropower projects were conducted by the Water and Power Consultancy Services (WAPCOS 1990) and the

Ministry of Water Resources (MOWR 1998), there is still a discrepancy in the estimates of hydropower potential under different flow and operational conditions and a lack of understanding on how this capacity can be best utilized under future climate conditions.

To consider climate change into water resources planning and management in the basin, an analysis of possible changes in multiple aspects of water resources under changing climatic conditions is required. This report aims to examine the future variability of hydrologic regimes and water resources of the Upper Blue Nile River Basin and the potential impacts in the basin and to downstream countries.

The Upper Blue Nile River Basin

Physiography

The Upper Blue Nile River Basin is located in the Ethiopian Highlands and has a drainage area of about 176,000 square kilometers (km^2) upstream of *El Diem* and comprises of six sub-basins (Figure 1). The river originates in Lake Tana and flows to the Sudanese *Border* to eventually meet the White Nile River at Khartoum, Sudan.

The climate of the study area varies from humid to semiarid. Most precipitation occurs in the wet season called *Kiremt* (from June to September). The two other seasons are known as *Bega* (normally dry; from October to February) and *Belg* (normally mild; from March to May). The seasonal precipitation based on data from 1961 to 1990 (Kim et al. 2008) shows about 240 millimeters (mm), 990 mm, and 190 mm in *Belg*, *Kiremt*, and *Bega*, respectively. About 70% of annual precipitation is concentrated on *Kiremt*. The annual precipitation has an increasing trend from northeast to southwest. The estimated mean annual precipitation of the study area ranges from 1,200 to 1,600 mm based on data from 1961 to 1990 depending on the studies (Gamachu 1977; Conway 1997; Conway 2000; Tafesse 2001; UNESCO 2004; Kim et al. 2008). The mean annual temperature estimated using the records from 1961 to 1990 is 18.3°C with a seasonal variation of less than 2°C (Kim et al. 2008). The annual potential evapotranspiration is 1,100 mm with a seasonal variation of less than 20 mm (Gamachu 1977; Kim et al. 2008). Both cited studies used the Thornthwaite method based monthly temperature data from 1965 to 1969 and from 1961 to 1990, respectively.

Due to the summer monsoon occurring between June and September, more than 80% of the annual flow occurs from July to October and flows to the downstream countries due to the absence of storage capacity. Small tributaries in the mountainous region experience large fluctuations of streamflow due to the seasonal variation of precipitation (UNESCO 2004). The monthly discharge time series at *El Diem*, which is the main outlet of the basin, between 1921 and 1990, taken from the National Center for Atmospheric Research (NCAR, http://dss.ucar.edu/datasets/, accessed in March, 2006), produce a mean annual discharge of 49 cubic kilometers (km^3) with a minimum of 31 km^3 (between 1972 and 1984) and a maximum of 70 km^3 (1929). The estimates of mean annual discharge at the same location from previous studies range from 46 to 54 km^3 due to the difference in recording periods and the number of data points (Conway 1997, 2000; Sutcliffe and Parks 1999; NMSA 2001; UNESCO 2004; Conway 2005).

Cultivated areas, woodlands, and grasslands/shrublands occupy about 60%, 25%, and 7%, respectively, of the Upper Blue Nile River Basin (Dr. Terekegn Deksyos, MOWR, pers. comm., April, 2006). The most common land use patterns are grazing and rain-fed agriculture, and as a result soil erosion is a big issue for the entire basin (UNESCO 2004).

Data

There are few reliable meteorological and hydrologic stations in the basin and most of the monitoring was started by NMSA and MOWR of Ethiopia in the early 1960s (Conway 2000). Monthly precipitation data from 10 stations (also used in previous studies of Johnson and Curtis 1994; Conway 1997,2000; Seleshi and Zanke 2004; Figure 1) were collected from the Global Historical Climatology Network (GHCN, ftp://ftp.ncdc.noaa.gov/pub/data/ghcn/v2/, accessed in March, 2006). Monthly temperature data for the period of 1961 to 1990 at eight of the ten stations (Figure 1, excluding Bahar Dar and Sibu Sire) were also collected from the GHCN. The missing precipitation and temperature data at each station were filled using local regression and correlation weight methods (Kim et al. 2008; Kim and Kaluarachchi 2008a). These climate variables were spatially averaged for each sub-basin and also for the entire basin using the Thiessen method.

The flow data available for this study included monthly discharge time series for stations 2001 (drainage area of 66,000 km^2, Figure 1) and *El Diem* and were collected from MOWR (Dr. Terekegn Deksyos, MOWR, pers. comm., April, 2006) and the NCAR, respectively.

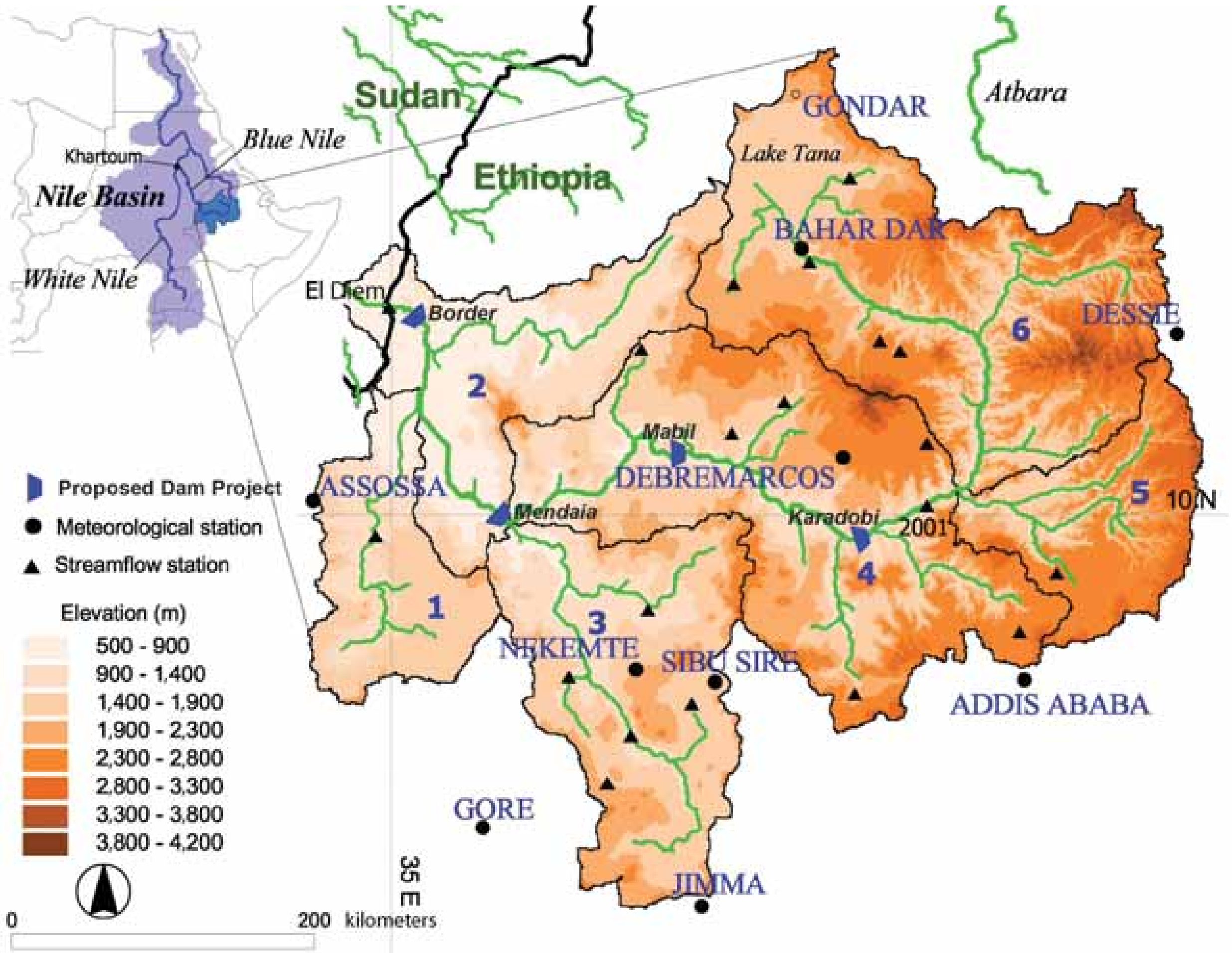

FIGURE 1. Physical layout of the Upper Blue Nile River Basin. Six sub-basins are presented in bold numbers. Digital maps were collected from the US Geological Survey's Center for Earth Resources Observation and Science (EROS) (available at http://edc.usgs.gov/products/elevation/gtopo30/hydro/africa.html (accessed in March, 2006)) and MOWR (Dr. Terekegn Deksyos, pers. comm., April, 2006).

Climate Scenarios

Baseline Climate Scenario

The baseline climate scenario represents current climate conditions. As in most of the previous climate change studies in this region, the baseline scenario is described using monthly precipitation and temperature for the period from 1961 to 1990. The conditional generation method (CGM) proposed by Kim et al. (2008) was used to extend the current precipitation time series to accommodate climate change effects while preserving the corresponding temporal and spatial correlation structures. The CGM is based on the historical relationship (conditional probability) between any two precipitation (or temperature) events. By conditioning a set of uniform random numbers to have this conditional probability, the CGM can generate the conditioned random numbers containing the historical relationship between two events. By doing so, the CGM generates the similar correlation structure to the observed regardless of the strength of correlation between the two observed precipitation events. The procedure using the CGM was used to develop the baseline temperature profile as well. Readers are encouraged to refer to Kim et al. (2008) for further information on the methodology.

For the baseline precipitation and temperature scenarios, 100-year monthly time series from the current conditions for the 10 stations (8 for temperature) have been generated using the CGM (Kim et al. 2008; Kim and Kaluarachchi 2008b). The baseline potential evapotranspiration scenario was then generated using the baseline temperature scenario by the Thornthwaite method (Palmer and Havens 1958). Although the Thornthwaite method has limitations due to its empirical nature, this study used this method due to the simplicity of data requirement.

Future Climate Scenarios

Each general circulation model (GCM) has different temporal and spatial resolutions and assumptions describing atmospheric processes. High uncertainty is, therefore, expected in climate change impact studies if the simulation results of a single GCM are relied upon (IPCC 1999). Hence, this study used the outputs of six different GCMs from the IPCC DDC (Data Distribution Center) to predict the precipitation patterns for the 2050s (mean of GCM results for the years 2040-2069). The GCMs used are CCSR/NIES (Center for Climate System Research and National Institute for Environmental Studies), CGCM2 (Canadian Global Coupled Model 2), CSIRO (Commonwealth Scientific and Industrial Research Organization), ECHAM4 (European Centre Hamburg Model 4), GFDL-R30 (Geophysical Fluid Dynamics Laboratory's Rhomboidal 30 truncation), and HadCM3 (Hadley centre Climate Model 3). Kim et al. (2008) used these six GCMs to construct future precipitation scenarios in the Upper Blue Nile Basin for the 2050s.

The mean monthly changes in precipitation (%) and temperature (°C) up to the 2050s simulated by these six GCMs were downloaded form the IPCC Data Distribution Center (http://ipcc-ddc.cru.uea.ac.uk/, accessed in April, 2006). This study adopted the A2 emission scenario (high emission scenario) described in the Special IPCC Report on Emissions Scenarios (see Chapter 5, IPCC 2000), which is a frequently used scenario for the mid to high range of emissions (e.g., Hulme et al. 2001; Conway 2005; Wilby and Harris 2006). The A2 scenario assumes a high population growth rate and a significant shift to coal in year 2100.

To properly manage the entire study area, four to nine grids were selected depending on the GCM. The mean monthly changes in precipitation and temperature of these selected grids were then spatially downscaled to the selected stations using the triangular cubic interpolation method (Watson 1992). The outputs of the six GCMs were then weighted based on their accuracy to simulate the current patterns (1961 to 1990) of precipitation and temperature for the study area (Table 1). To find the weights in Table 1, the monthly distributions of the 1961-1990 precipitation and temperature simulated by the six GCMs were compared with the observed data. The mean absolute errors of individual GCMs were then inversely weighted so that a GCM showing a smaller error can have a larger weight.

The reason for this weighting is that it is normally difficult to select a specific GCM for the area of interest. This weighted scenario can, therefore, suggest an ensemble average projection for climate change from these six GCMs. The total number of climate scenarios is now seven (six scenarios from the outputs of individual GCMs and one weighted scenario) for both precipitation and temperature.

Future climate variables, precipitation and temperature, were constructed for each climate scenario by perturbing the corresponding baseline precipitation or temperature data series with the predicted changes in precipitation from a given GCM. This perturbation method has been widely used in previous climate change studies (e.g., Conway and Hulme 1996; Yates and Strzepek 1998b; Xu 2000; Fowler et al. 2003; Kim et al. 2004; Drogue et al. 2004; Wurbs et al. 2005). The major assumption of this method is that the current temporal and spatial correlation structures of precipitation and temperature will be preserved over time.

TABLE 1. Description of the six GCMs used in this study.

GCM	Country	Resolution[a]	Sensitivity (°C)[b]	Grids used[c]	Weight[d] (%)	
					P	T
CCSR/NIES	Japan	5.625, 5.533	3.5	4	19	2
CGCM2	Canada	3.750, 3.709	3.5	9	7	20
CSIRO	Australia	3.625, 3.184	4.3	6	25	4
ECHAM4	Germany	2.813, 2.789	2.6	9	10	18
GFDL-R30	USA	3.750, 2.235	4.0	9	6	4
HADCM3	UK	3.750, 2.500	2.5	9	33	52

[a] Average resolution of each GCM (longitude, latitude).
[b] Sensitivity is the increase of temperature from the baseline (1961-1990) due to doubling of CO_2.
[c] The number of grids covering the study area.
[d] Weights for precipitation (P) and temperature (T) computed by Kim et al. (2008) and this study, respectively.

Runoff Generation

This study used a simplified monthly water balance model (Figure 2) due to limited data availability from the study area. This model transforms precipitation and potential evapotranspiration through two soil moisture storage zones into runoff. In Figure 2, KD, K1, K2, KI, and KL, are the coefficients [T^{-1}] for direct runoff (QD), surface runoff (Q1), base runoff (Q2), infiltration (I), and percolation (L), respectively. H1 and H2 are the heights of runoff orifices in the upper and lower zone, respectively. IM is the fraction of impervious area. UZSM and LZSM, which are updated with water balance accounting, represent upper and lower zone soil moisture, respectively. Evapotranspiration is updated for each time step using the relationship between precipitation and potential evapotranspiration (Dingman 2002). Infiltration and deep percolation is also updated for each time step depending on the availability of soil moisture in each tank.

As described in the previous section, urbanization is minimal in the study area and, thus, the fraction of impervious area is negligible making parameters IM and KD insignificant. Therefore, a total of six calibration parameters (H1, H2, K1, K2, KI, and KL) are used. Maximum heights of two soil moisture storages can be determined from soil data of the basin (Kim and Kaluarachchi 2008a).

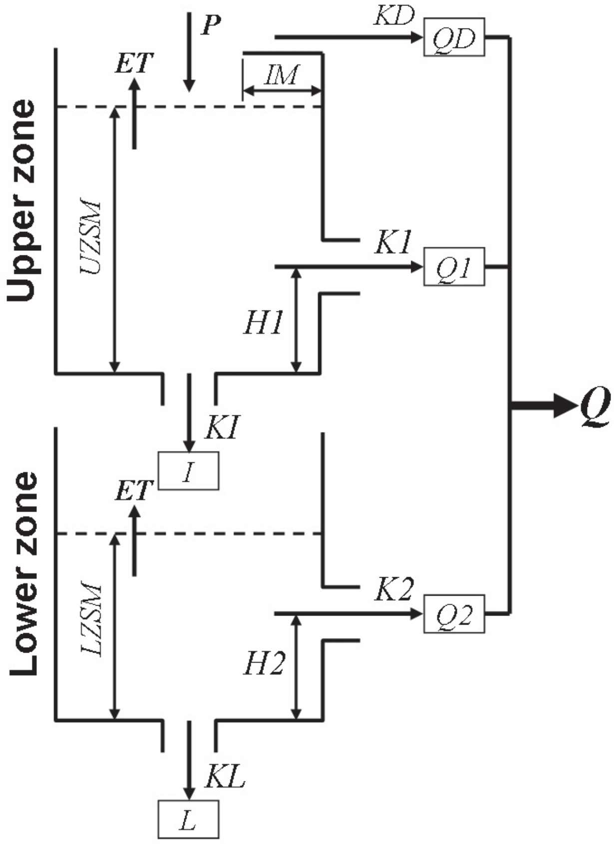

FIGURE 2. A schematic of the water balance model used in this study.

The six sub-basins of the study area (Figure 1) are ungauged and, therefore, traditional model calibration is not possible. The runoff volume from an ungauged sub-basin can be estimated using a regression relationship between total channel length and runoff. The total channel length of a sub-basin was computed using a stream network Geographic Information System (GIS) file. Since this estimated runoff volume is not very accurate, it is converted to a fraction of the total runoff volume at the *El Diem* outlet of the basin. Therefore, the sum of volume fractions of the six sub-basins should be equal to one. Using this runoff volume fraction, the hydrograph of each sub-basin is then computed by disaggregating the hydrograph at the basin outlet *El Diem* (Kim and Kaluarachchi 2008a). Finally, the model parameters of each sub-basin can be calibrated to the estimated hydrograph and are used to generate runoff of an ungauged sub-basin under different climate scenarios.

Monthly discharge data at stations 2001 and *El Diem* from 1961 to 1990 were used for model calibration (1961 to 1980) and verification (1981 to 1990) using the approach discussed in the earlier paragraph. As shown in Figure 3, the Nash and Sutcliffe (NS) coefficient values (Nash and Sutcliffe 1970) for the calibration and verification periods were 0.83 and 0.79 for station 2001 and 0.86 and 0.85 for *El Diem*, respectively. For the entire period, NS coefficients were 0.82 and 0.86 for Station 2001 and *El Diem*, respectively. The model calibration work was similar to the work of others (Conway and Hulme 1996; Yates and Strzepek 1996; Yates and Strzepek 1998a,b) assuming that the model parameters would not significantly vary with time. The same assumption was made with potential land use changes as well.

The water balance model was run for each climate scenario (the baseline scenario, six GCM scenarios, and the weighted scenario) using the model parameters calibrated and regionalized for the six sub-basins.

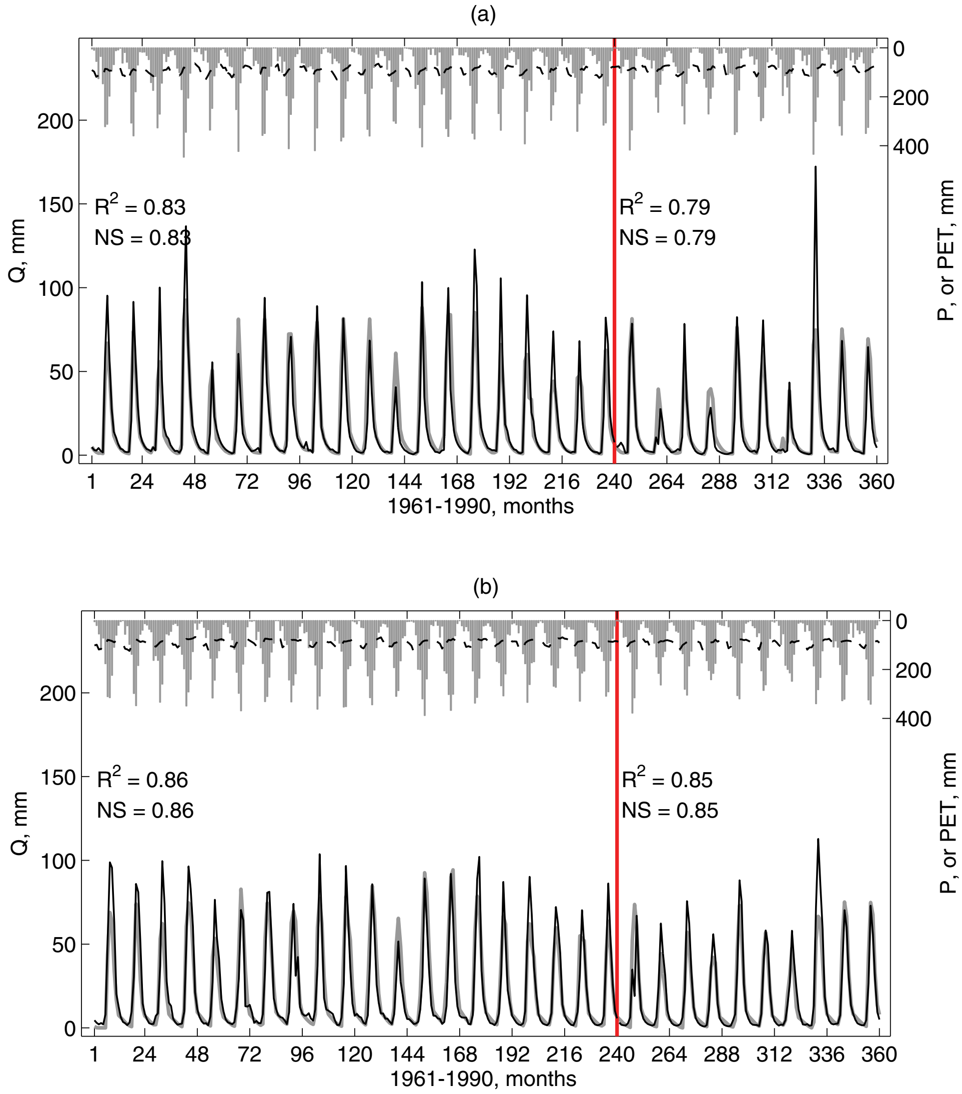

FIGURE 3. Monthly runoff hydrographs at (a) Station 2001, and (b) *El Diem*.

Impacts of Climate Change

Hydrology

Runoff was simulated using the climate inputs from different climate scenarios (baseline, weighted GCM scenario as a mean, and six GCMs). The results in Table 2 suggest that the changes in mean annual precipitation from the six GCMs range from -11% by CSIRO to 44% by CCSR/NIES with a change of 11% from the weighted average scenario. On the other hand, the changes in mean annual temperature range from 1.4°C by CCSR/NIES to 2.6°C by HadCM with a change of 2.3°C from the weighted average scenario. Potential evapotranspiration shows an increasing trend for all GCMs due to increased temperature. The changes in potential evapotranspiration are from 9% by CCSR/NIES to 19% by HadCM3 with a change of 16% from the weighted average scenario. The reason is that CCSR/NIES simulates the wettest and coolest scenarios and HadCM3 simulates the warmest scenario (Table 2).

TABLE 2. Changes in climate variables and runoff for the 2050s in the study area.

GCM	△P (%)	△T (°C)	△PET[a] (%)	△Q[a] (%)
Weighted scenario	11	2.3	16	4
CCSR/NIES	44	1.4	9	80
CGCM2	-3	1.7	11	-14
CSIRO	-11	2.1	14	-32
ECHAM4	33	2.4	17	64
GFDL-R30	1	1.7	11	-13
HadCM3	6	2.6	19	-11

[a] PET and Q represent potential evapotranspiration and runoff, respectively.

Simulated hydrologic response of the basin under different climatic conditions produced by each GCM is presented in Figure 4 for the 2050s. It is observed that the CCSR/NIES and ECHAM4 scenarios produced biased mean monthly runoff distributions between July and December. This is coincident with the overpredicted precipitation for the same period by CCSR/NIES and ECHAM4 compared to other GCMs (Kim et al. 2008). The simulation results suggest that the changes in mean annual runoff are from -32% by CSIRO to 80% by CCSR/NIES with an average change of 4%. As indicated by Yates and Strzepek (1998a,b), the changes in basin runoff are controlled not only by precipitation but also by temperature and potential evapotranspiration. For example, in Table 2, the change in mean annual runoff was simulated as -14% by CGCM2 which is a 3% decrease in mean annual precipitation and 1.7°C increase in mean annual temperature. On the other hand, the -11% change in mean annual runoff was simulated by HadCM3 which produced a 6% increase in mean annual precipitation and a 2.6°C increase in mean annual temperature.

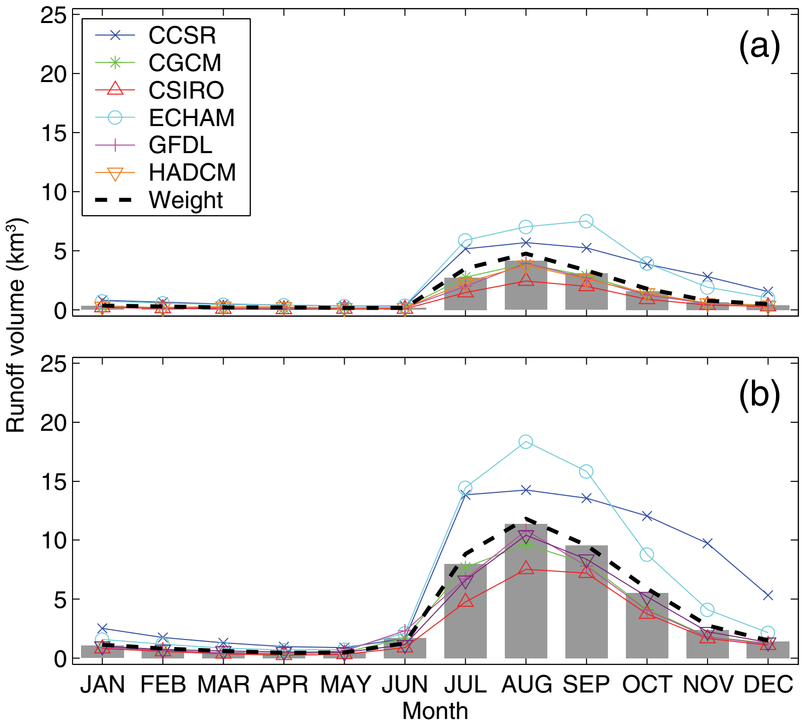

FIGURE 4. Comparison of the mean monthly runoff distributions at (a) Station 2001, and (b) *El Diem* under different climate scenarios for the 2050s. The bars represent the baseline runoff.

When compared to the results of previous studies for the same area (see Table 3), the changes simulated by the weighted scenario in this study (11% in precipitation, 2.3°C in temperature and 4% in runoff) can be classified as mild increases. The relationship between the changes in runoff and the changes in precipitation and temperature was developed by regression using the changes of six sub-basins (i.e., 36 (6 sub-basins * 6 GCMs) of ΔQ scenarios as a dependent variable and also 36 of ΔP and ΔT scenarios as independent variables), using the six GCM outputs, and is given as:

$$\triangle Q = 2.2 \times \triangle P - 7.5 \times \triangle T \qquad (1)$$

where: $\triangle Q$ is the percentage change in mean annual runoff; $\triangle P$ is the percentage change in mean annual precipitation; $\triangle T$ is the °C change in mean annual temperature; and the coefficient of determination of this equation is 0.97.

This relationship is useful to predict the mean changes in runoff of the study area due to climate change. The validity of equation (1) was evaluated by applying this equation to previous studies and the results are presented in Table 3. As presented in the last column of Table 3, the mean annual runoff changes (%) predicted by equation (1) show a good agreement with those by previous studies (a correlation coefficient of about 0.99). However, equation (1) may produce unfeasible results, if applied to small catchments within sub-basins, because this relationship was derived using hydrologic responses at sub-basin scale.

The average changes of climate variables and runoff from the six sub-basins are shown in Figure 5. Compared to the southwest of the study area, the northeast shows a more pronounced increasing trend in precipitation and a less pronounced increasing trend in temperature. These trends result in a noticeable increase in runoff in the northeast compared to the southeast. The northeast includes the *Amahara* region, one of the most populated and agricultural regions of Ethiopia. It is also noted that the sub-basin 1, in which the *Dabus* swamps are located, shows a large decrease in runoff due to increased temperature and potential evapotranspiration in this region.

Table 3. Changes in climate variables and runoff projected for the Upper Blue Nile River Basin by previous studies.

		Result				
Study	GCM used	△P (%)	△T (C)	△Q (%)	Condition	△Q (%) by Equation (1)
Conway and	GFDL	-2	0.7	-9	2025	-9
Hulme (1996)	GISS[a]	7	0.8	15	2025	10
	Composite	2	1.0	1	2025	-3
Yates and	GFDL	-5	3.5	-	2030s	-
Strzepek (1996)	GISS	47	3.4	-	2030s	-
Yates and	GFDL	4	2.9	2	2xCO_2	-13
Strzepek (1998b)	GFDLT[b]	-5	2.9	-31	2050s	-33
	GISS	39	3.4	108	2xCO_2	60
	UKMO[c]	55	3.7	133	2xCO_2	92
	MPI[d]	23	2.2	43	2xCO_2	35
	CGCM	-9	2.4	-35	2xCO_2	-37
Yates and	GFDL	-5	3.5	-	2xCO_2	-
Strzepek (1998a)	UKMO	29	4.8	-	2xCO_2	-
	GISS	30	2.2	-	2050s	-
NMSA (2001)	CGCM	-	-	-33	2xCO_2	-
	GFDL	-	-	-3	2xCO_2	-
	UKMO	-	-	10	2xCO_2	-

[a] GISS: Goddard Institute for Space Studies.
[b] GFDL Transient scenario for the 2050s.
[c] UKMO: United Kingdom Meteorological Office.
[d] MPI: Max Plank Institute for Meteorology.

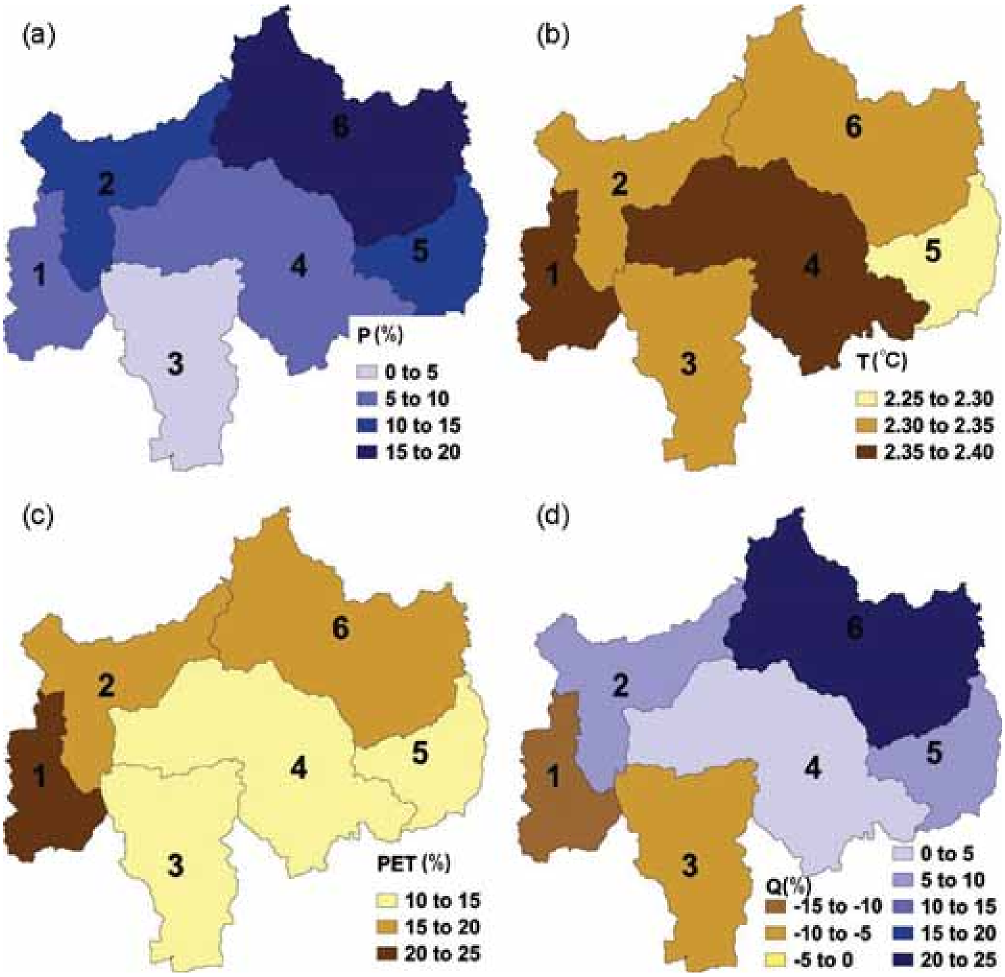

Figure 5. Spatial distribution of the average annual changes in climate variables and runoff under the weighted scenario for the 2050s: (a) precipitation, (b) temperature, (c) potential evapotranspiration, and (d) runoff.

Flow regimes in a basin can be effectively quantified using flow statistics based on flow duration curves. Since flow duration curves at a specific location represents the relationship between the magnitude and frequency of daily, weekly, or monthly (or other timescales) streamflow, they can provide a simple, yet comprehensive, view of the overall flow variability in a basin (Vogel and Fennessey 1994; Smakhtin 2001). Vogel and Fennessey (1994) showed that flow duration curves are sensitive to the hydrologic extremes associated with the particular period of records chosen. To overcome this problem, this study adopted the medians of 30-year flow duration curves derived from the simulated 100-year monthly hydrographs corresponding to the baseline and future runoff scenarios from the six GCMs.

To assess the changes in flow regimes, the flow statistics that represent high, median, and low flows were extracted from the flow duration curves of the six sub-basins and the basin outlet. These flow statistics are termed Q_{10}, Q_{50}, and Q_{90} and define the flows exceeding 10, 50, and 90% of the time, respectively. The mean flow, Q_m, was also computed because the hydropower generation capacity is a function of the mean flow at a given hydraulic head. In addition, the periods (the number of months) above Q_{10} and below Q_{50}, Q_{90}, and Q_m, which are termed here as D_{10}, D_{50}, D_{90}, and D_m, respectively, were computed to investigate how frequently these events occur. The changes in outflow patterns from the potential future dams, *Karadobi* and *Border*, were also evaluated using the hypothetical dam operation policies that will be described next.

Figure 6 presents the percentage changes in flow statistics (Q_{10}, Q_{50}, and Q_{90}) of the six sub-basins under the weighted runoff scenario for the 2050s. While Q_{10} and Q_{50} show a similar range of percentage changes (-15% to 20%), the range of changes in Q_{90} is much wider (-25% to 60%). This result can be explained by runoff in low-flow seasons, which is usually more sensitive to changes in potential evapotranspiration than runoff during high-flow seasons. It is also partially because a relative percentage change value is magnitude-sensitive, e.g., the same increment or decrement gives a higher percentage change for low flows than for high flows. An increasing trend of these three flow statistics towards the northeast is generally a coincident with that of the mean annual runoff (Figure 5d). The increased low flows in this region suggest the increased baseflow during the mild *Belg* season (February through May).

The increased flows during the *Belg* season need to be analyzed further. Low flows dominate the period from February to May (Figure 4). Analysis of the 70-year monthly discharge data available at *El Diem* suggests that minimum annual flow occurs mostly in April (59%) and March (25%). In addition, Kim and Kaluarachchi (2008a) described the half-time of flow depletion, which defines the time for flow to halve in a receding limb of a hydrograph (Martin 1973), in the study area to be about 4 months. These two observations suggest that runoff in March through April can be strongly controlled by the quantity and timing of precipitation from November to February (*Bega* season) of the previous year. Combining these observations with the results that the percentage change in *Bega* precipitation is higher than in *Kiremt*'s or *Belg*'s (Kim et al. 2008), a higher percentage increase in the low flow (Q_{90}) than in the high flow (Q_{10}) is feasible (Figure 6c and the K0+B0 case of Table 5 to be discussed next).

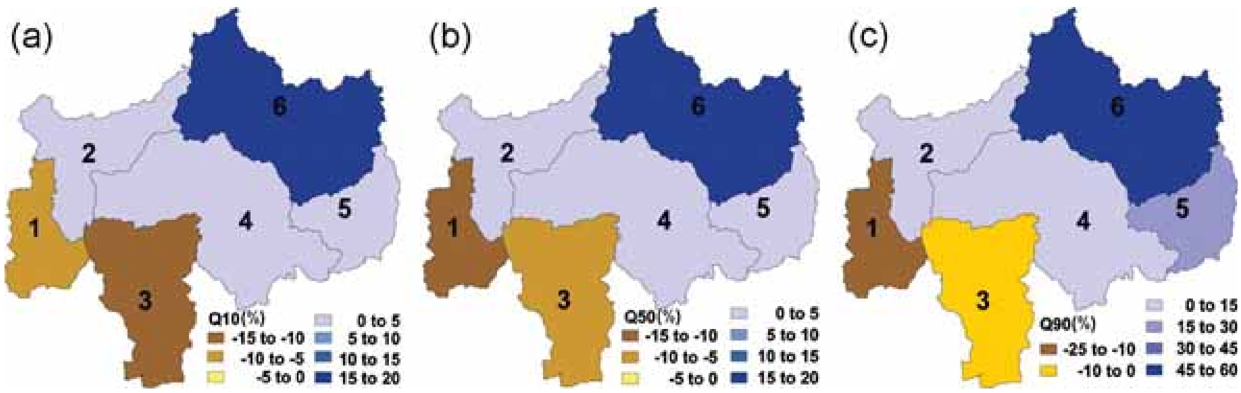

FIGURE 6. Spatial distribution of the percentage changes in flow statistics under the weighted runoff scenario for the 2050s.

Drought Analysis

Ethiopian agriculture depends completely on precipitation. Therefore, precipitation variability and droughts in particular affect food security in the study area (Conway 2005). A meteorological drought is characterized using various drought indices, of which the Standardized Precipitation Index (SPI, McKee et al. 1993) is most widely used. SPI quantifies precipitation deficits at various timescales based on the probability of recording a given amount of precipitation, and the probabilities are standardized so that an index of zero indicates the median precipitation amount. The index is negative for drought, and positive for wet conditions. Guttman (1998) and Hayes et al. (1999) found that the SPI has advantages of statistical consistency and the ability to describe both short- and long-term drought impacts through different timescales of precipitation anomalies. SPI values with various timescales can, thus, reflect the impacts of drought on different components of water resources such as soil moisture, groundwater, or river flow.

In this study, SPI values for 1-, 3-, 6-, 9-, and 12-month timescales were computed using observed monthly precipitation at 10 stations from 1961 to 1990 to determine which timescale better represents the historical drought events of the study area. Although SPI1, SPI3, and SPI6 all captured historical drought events, the analysis showed that SPI1 and SPI3 values were found to be too sensitive to variations in short-term precipitation deficit while the SPI6 was determined to be more suitable to assess mid- to long-term droughts. Therefore, the 100-year SPI6 series of the six sub-basins were computed for each future precipitation scenario and compared with those from the baseline precipitation scenario.

Frequency, duration, and severity are the important characteristics of a drought. To consider these factors, this study counted the number of severe drought events based on six-month duration of precipitation, i.e., SPI6 values less than -1.5 defined by McKee et al. (1993). The percentage changes of frequencies in SPI6 values of less than -1.5 were computed for future precipitation scenarios, relative to those derived from the baseline precipitation scenario. As shown in Table 4, the percentage changes in severe drought events vary significantly depending on the GCM. In the weighted precipitation scenario, which provides the ensemble average of all GCM scenarios, the percentage changes in severe drought frequencies are about -90% for sub-basins 5 and 6, about -70% for sub-basins 2 and 4, and -30 to -50% for sub-basins 1 and 3.

Water Resources Reliability

A quantitative measure of performance of water resource systems is useful in assessing the operational strategies of the potential future dam projects. Hashimoto et al. (1982) suggested the use of indices of reliability, resiliency, and vulnerability, for classifying and assessing the performance of water resource systems. *Reliability* is a measure of frequency or probability that a system is in a satisfactory state meeting a given criterion. *Resiliency* generally indicates a measure

TABLE 4. Percentage changes of frequencies in SPI6 values of severe drought events for the 2050s.

GCM	Sub-basin					
	1	2	3	4	5	6
Weighted scenario	-50	-74	-31	-73	-86	-92
CCSR/NIES	-76	-84	-33	-88	-90	-88
CGCM2	81	46	162	114	83	-31
CSIRO	85	202	117	238	321	421
ECHAM4	-19	-45	-49	-82	-92	-85
GFDL-R30	73	52	25	23	6	-21
HadCM3	-39	-47	-37	-34	-47	-63

of how quickly a system recovers from failure once failure has occurred. *Vulnerability* can be defined as (1) the maximum duration of system failure; and (2) the cumulative maximum magnitude of water shortage during a system failure. The computational scheme for these indices in this study is almost similar to that of Hashimoto et al. (1982), Maier et al. (2001), and Fowler et al. (2003), except for the use of a monthly time step and a different criterion.

Defining a criterion (*C*) as the minimum required runoff from a water resource system (river or dam outflow), the monthly runoff (X_t) at time t can be classified as a satisfactory state (*S*) or a failure state (*F*), i.e.,

$$\text{If} \quad X_t \geq C \quad \text{then} \quad X_t \in S \quad \text{and} \quad Z_t = 1 \qquad \text{else} \quad X_t \in F \quad \text{and} \quad Z_t = 0 \tag{2}$$

where: Z_t is a generic indicator variable. The mean monthly runoff distribution of the baseline runoff scenario was used as a criterion and, thus, system failure occurs when runoff or outflow is below the criterion at any given month. Another indicator, W_t, which represents a transition from *F* to *S*, is defined as:

$$W_t = \begin{cases} 1, & \text{if} \quad X_t \in F \quad \text{and} \quad X_{t+1} \in S \\ 0, & \text{otherwise} \end{cases} \tag{3}$$

If the periods of X_t in *F* are defined as U_1, U_2, …, U_N where *N* is the number of *F* periods, then reliability, resilience, and vulnerability indices during the total time period (*T*) can be defined as:

$$\text{Reliability} = \frac{\sum_{t=1}^{T} Z_t}{T} \tag{4}$$

$$\text{Resiliency} = \frac{\sum_{t=1}^{T} W_t}{T - \sum_{t=1}^{T} Z_t} \tag{5}$$

$$\text{Vulnerability}_{\text{Time}} = \max\{U_1, U_2, \ldots, U_N\} \tag{6}$$

$$\text{Vulnerability}_{\text{Volume}} = \max\left\{\sum_{t \in U_i} (C\text{-}X_t), i = 1, 2, \ldots, N\right\} \tag{7}$$

These indices were previously used to evaluate reservoir operations (Hashimoto et al. 1982; Moy et al. 1986) and water distribution systems (Zongxue et al. 1998); manage water quality of a river (Maier et al. 2001) as well as assessing climate change impacts on water resource systems (Fowler et al. 2003). This study examined the percentage changes in these indices computed for future runoff scenarios associated with potential future dam operation policies, relative to those computed for the baseline runoff scenario. Therefore, these percentage changes can suggest the impacts of both climate change and dam operation on the robustness of water supply.

First, this section evaluates the impacts of climate change on reliability, resiliency, and vulnerability of streamflows in sub-basins under the unregulated (natural) condition. The reliability and resiliency under the weighted runoff scenario for the 2050s suggest that there is an increasing trend towards the northeast (Figures 7a and 7b). This improved water supply capability in this region, therefore, results in the decreased frequency of system failure measured by reliability and increase of system flexibility measured by resiliency.

Although the increased runoff generally improves water supply reliability, the vulnerability of streamflows can be dominated by the timing and duration of runoff. In the case of sub-basin 5, the vulnerability in maximum failure time is not decreased in spite of its increased runoff. Increased vulnerability (Figures 7c and 7d) as well as decreased reliability and resiliency (Figures 7a and 7b) is expected in the southwest region, sub-basins 1 and 3, due to the reduced runoff (Figures 5d and 6b). Particularly, more than a 50% increase in maximum water shortage in a failure period (Figure 7d) can cause a severe water supply problem in those sub-basins.

However, runoff from the entire basin measured at *Border* shows an improved capability of water supply to downstream countries. Although changes are dependent on a specific GCM, the weighted runoff scenario for the 2050s suggests that the assessment indices of natural runoff at *Border* are improved and will be discussed in the next section, *Hypothetical Dam Operations for*

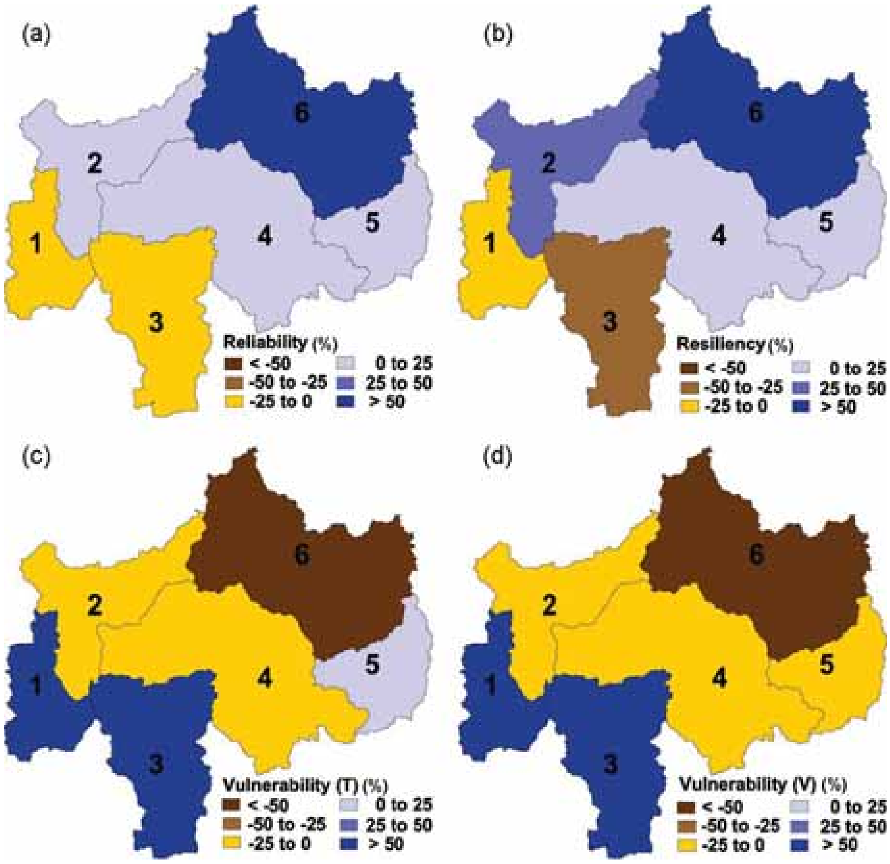

FIGURE 7. Spatial distribution of the percentage changes in water resources assessment indices reliability, resilience, and vulnerability for volume and time of streamflows under the weighted runoff scenario for the 2050s.

Hydropower. The increased reliability and resiliency of flows are beneficial to both the study area and downstream countries because hydropower generation in the study area could be stable and the likelihood of water supply failure to downstream countries could be reduced.

Hypothetical Dam Operations for Hydropower

This section mainly analyzes the impacts of hydropower generation under the climate change scenarios on streamflow variability at the basin outlet. The 100-year monthly hydrographs from sub-basins 5 and 6 were aggregated as inflow to the *Karadobi* Dam and those from all six sub-basins were aggregated as inflow to the *Border* Dam. Block (2007) discussed potential future dam sites in the region for hydropower generation. Although these sites are not officially proposed or under discussion by the Ethiopian or other riparian countries, two dam sites were selected from the construction as priority and discussed by Block (2007). Therefore, these hydropower dam sites should be considered hypothetical at the present time. Based on the information presented in MOWR (1998) and Block (2007), the maximum capacity of each dam was assumed to be 1.6 and 0.3 times of the mean annual runoff volume of the baseline runoff scenario for Station 2001 and *El Diem*, respectively. With mean annual runoff volumes of 14 and 43 km^3, the maximum capacities of each dam are 22.4 and 12.9 km^3 at Station 2001 and *El Diem*, respectively.

The operational performance of a water resources system greatly depends on the timing and quantity of streamflow at the site of interest. The constraint functions not only prescribe how the proposed dams may be filled and the optimal allotment to irrigation, but also allow for the assessment of potential impacts on downstream countries (Block 2007). In this study, however, the allotment of streamflow to irrigation was not considered due to the lack of reliable information. This diversion for irrigation can be easily performed in a future study as long as necessary information is available. The initial storage of each dam for the 2050s was assumed to be 70% of its maximum capacity. The assumed capacity of each dam is slightly less than that proposed by MOWR (1998) because the discharge data used in this study are different from those of previous studies. This underestimated capacity is conservative for the operation of the dams under future irrigation consumption and climate variability. This analysis did not consider the potential impacts of sediment generation and transport through different dam operation policies.

The dams at *Karadobi* and *Border* were originally proposed for hydropower generation. Therefore, the hypothetical dam operation policies described in this study only assume hydropower generation without any consumptive water uses such as irrigation or water transfer. The first dam operation policy, denoted as K1 and B1 for *Karadobi* and *Border* sites, respectively, allows 5% of annual runoff volume at *Border* to be impounded within the basin (at one or both dams based on single or joint operation) using the mean monthly flow of the baseline runoff scenario. The second operation policy denoted as K2 and B2 for *Karadobi* and *Border* sites, respectively, allows only an excess of monthly runoff above a threshold (mean monthly flow of the baseline runoff scenario) to be impounded in each dam. The third policy denoted as K3 and B3 for the respective sites, allows supplemental releases to be made, when the monthly outflow is below the threshold of that month while satisfying the second policy as well.

The concepts of the first and second policies were originally proposed by Block (2007) on an annual basis. In this study, all policies were programmed on a monthly basis to reasonably account for the monthly variation of runoff in a year. In addition to Block (2007), this study proposes the third policy to effectively mitigate the intra-annual natural runoff fluctuations (i.e., below the historical mean monthly flow) which can frequently occur in the second policy without supplemental releases. For flood control and dam safety, the inflow exceeding the maximum capacity of each dam is released during simulations.

Both single and joint dam operations were assessed to find the best combination of policies that can maximize the hydropower generation and available water resources for both the study area and downstream countries. All operational polices proposed earlier can be combined to define various dam operation combinations for each dam. Therefore, combinations can be one case of no dam operation (K0+B0), six cases of single dam operation (K1+B0, K2+B0, K3+B0, K0+B1, K0+B2 and K0+B3), and nine cases of joint dam operation (K1+B1, K2+B1, K3+B1, K1+B2, K2+B2, K3+B2, K1+B3, K2+B3 and K3+B3). As discussed in Block (2007), none of these policies are, presently, legally acceptable under the 1959 Agreement between Ethiopia and Sudan or Egypt.

For the ‘no dam condition’ based on the weighted runoff scenario for the 2050s in Table 5, the low-flow statistic (Q_{90}) shows a large increase, thus implying a wetter dry season for the study area. On the other hand, the slightly increased high-flow statistic (Q_{10}) indicates that the flood risk to downstream countries may become higher than current climate conditions. The mean flow (Q_m) shows a 5% increase for the 2050s while the median (Q_{50}) was simulated to be rarely changed. A slight increase in hydropower generation could be possible with the increased mean flow. The low-flow period (D_{90}) is reduced by 27%, while the high-flow period (D_{10}) is increased by 22%. On the other hand, D_{50} and D_m are rarely changed.

The weighted runoff scenario was used as the representative runoff for the 2050s. Although not shown here for all cases, the K1+B0 and K0+B3 cases performed best amongst the six cases of single dam operation for each dam, and the K1+B3 case performed best amongst the nine cases of joint dam operation. Table 5 presents the percentage changes in assessment indices and flow regimes at the *Border* Dam location for the 2050s.

TABLE 5. Percentage changes in water resources assessment indices and flow regimes at the *Border* site for the 2050s.

Case	GCM	Assessment index[a] (%)				Flow (%)				Period (%)			
		REL	RES	VUL_T	VUL_V	Q_{10}	Q_{50}	Q_{90}	Q_m	D_{10}	D_{50}	D_{90}	D_m
K0+B0	Weighted	25	31	-12	-14	4	-1	14	5	22	1	-27	-2
	Max[b]	102	385	424	1,062	67	165	142	80	258	22	114	8
	Min[c]	-91	-84	-84	-91	-29	-28	-35	-32	-91	-44	-97	-25
K1+B0	Weighted	4	18	-28	-6	1	-5	6	2	4	4	-13	-2
	Max	101	374	568	1,451	64	153	127	75	237	23	123	9
	Min	-93	-86	-80	-91	-31	-31	-38	-34	-88	-42	-97	-25
K0+B3	Weighted	75	31	-68	-77	-4	0	3	3	-7	5	-64	0
	Max	112	421	76	237	44	57	53	40	140	16	94	6
	Min	-55	-42	-100	-100	-10	-22	-35	-18	-37	-17	-100	-11
K1+B3	Weighted	70	37	-64	-74	-4	0	3	3	-9	5	-56	0
	Max	112	421	76	247	44	55	55	40	134	17	97	6
	Min	-56	-44	-100	-100	-12	-23	-36	-18	-39	-15	-100	-11

[a] REL, RES, VUL_T, and VUL_V represent reliability, resiliency, vulnerability of time duration, and volume in system failure, respectively.
[b, c] Maximum and minimum values from simulated results under the six GCM scenarios.

In general, the results in Table 5 suggest that *Border* Dam operation (the K0+B3 case) performs better than *Karadobi* Dam operation (the K1+B0 case) although the K1+B0 case also shows an improvement to the baseline runoff scenario. First, the reliability and resiliency of water supply to downstream are noticeably increased by 75% and 31% (4% and 18% in the K1+B0 case), respectively. Second, the maximum water shortage and failure duration (i.e., vulnerability) are noticeably reduced by -68% and -77% (-28% and -6% in the K1+B0 case), respectively. Third, overall flow characteristics are improved. Q_{10} and D_{10} are decreased by -4% and -7% (1% and 4% increases in the K1+B0 case), respectively, and therefore the likelihood of flood risk is lower than the baseline runoff scenario and the K0+B0 case. Although the increases of Q_{90} and Q_m in the K0+B3 case are smaller than the K0+B0 case (no dam), the low-flow period (D_{90}) is significantly decreased due to the controlled releases from the *Border* Dam during low-flow seasons. A major reason for these superior improvements of the K0+B3 case rather than the K1+B0 case is that the K1+B0 case is less efficient in providing stable flows to downstream countries than the K0+B3 case. Recalling the operation policies, the K1+B0 case allows a 5% share of annual runoff at *Border* to be impounded in *Karadobi* regardless of intra-annual fluctuations (e.g., below the mean monthly runoff) while the K0+B3 case can mitigate those fluctuations by releasing supplemental outflows.

Although the best-performed joint dam operation (the K1+B3 case) displays an almost similar performance with the K0+B3 case, the K1+B3 case provides more beneficial aspects than the previous two cases based on the indices presented in Table 3. While depending on the GCMs (Table 5), the weighted runoff scenario for the 2050s suggests that, most of all, the hydropower potential will be significantly increased due to the two simultaneously operating dams.

Furthermore, the results of the K1+B3 case in Table 6 show that the mean annual water storage is larger than the other two cases while the outflow ratio (total outflow/total inflow) is not affected but increased from the baseline runoff scenario. The mean annual storage simulated by the K1+B0, K0+B3 and K1+B3 cases shows 55, 13, and 65% to the total capacity of the two dams, respectively. The K0+B3 case shows the lowest mean annual storage because of (1) supplementary releases of water during low-flow seasons, and (2) the *Border* Dam is smaller in capacity than the *Karadobi* Dam. The K1+B3 case obviously shows the largest mean annual storage by jointly operating two dams.

TABLE 6. Percentage of changes in mean annual water storages and outflow ratios simulated under the proposed operation policies for the 2050s.

Case	GCM	Storage (%)[a]	Outflow ratio (%)[b]
K0+B0	Weighted scenario	0	105
	Max	0	180
	Min	0	68
K1+B0	Weighted scenario	55	102
	Max	58	175
	Min	53	66
K0+B3	Weighted scenario	13	103
	Max	34	140
	Min	3	82
K1+B3	Weighted scenario	65	103
	Max	89	140
	Min	59	82

[a] Relative to the total capacity of two dams.
[b] Relative to the baseline runoff volume.

Another important issue that must be considered in any water management project proposed for the Nile Basin system is to assess the variability of total runoff volume from upstream countries. Under the weighted runoff scenario for the 2050s, the outflow ratios for the K0+B0 case (no dam) and the three cases, K1+B0, K0+B3 and K1+B3, are 105, 102, 103 and 103%, respectively, when using the baseline runoff scenario as the total inflow (Table 6). The three operation policies do not affect (increase or decrease) the runoff volume of the study area.

Current and future water abstractions from the two reservoirs or the main stem by Ethiopia could not be considered here because (1) these two potential future dams were proposed for hydropower generation (MOWR 1998), and (2) it is difficult to predict the exact amount of irrigation consumption of the study area for the 2050s due to the lack of reliable information. Based on the historical irrigation data of the Blue Nile Basin in Ethiopia, surveyed by the Food and Agriculture Organization of the United Nations (FAO 1997, Table 23), Kim and Kaluarachchi (2008b) has concluded that the proposed operation policies without water abstractions are acceptable for the two potential future dams by assuming that cultivated area of 21,000 ha in 1989 will increase five times by the 2050s.

Conclusions

This study is a step towards integrating climate change and hydrology of the Upper Blue Nile River Basin to assess the changes to water resources and the impacts due to potential dam operation policies in the 2050s. The study was conducted with limited hydrologic data and hence used simple, yet reliable, modeling approaches to simulate various impacts of climate change scenarios on hydrology and water resources of the basin. The major findings of the study include:

A generally increasing trend in both precipitation and runoff in the northern part of the study area, *Amhara*, is identified under the weighted scenario (combination of GCM outputs) for the 2050s. It is, therefore, possible to suggest that water availability will most likely improve in this area.

The standardized precipitation index (SPI), a commonly used measure of dryness/wetness over various time intervals, points to a reduction of severe drought events by 2050s in the study area due to increased precipitation. This observation indicates improved availability of water for agriculture. The identified augmented low-flows or reduced low-flow periods are also encouraging signs of improvement of the long-term food security during a dry season. Although a slight increase in flood risk is noted, it could most likely be handled in a timely manner. Joint dam operations (at both *Karadobi* and *Border*) under future climate scenarios will most likely provide more hydropower generation, enhance the duration of flows, and impound more water without affecting water availability to downstream countries. The dam capacity values used in this work were conservative and, therefore, the increased mean annual storage due to joint dam operation may be beneficial to agriculture and other users.

Climate change scenarios based on the GCMs are not the forecasts of future climate. However, simulated results for the 2050s can provide good insights to water resource planners for understanding the possible ranges and trends of climate change and their impacts. The results of hypothetical dam operations can inform decision-makers about possible ways of modifying the proposed dam operation policies in the future. Overall, the results suggest that the water resources of the Upper Blue Nile River Basin may not be adversely affected by climate change unlike many other regions in the world and that increases in precipitation and associated water resources may help to meet future water needs in the region. This work addressed hydrology and water resources of the Upper Blue Nile River Basin under limited data using simple yet a reliable hydrologic model. Although not discussed here, the results of the two-tank hydrologic model discussed by Kim and Kaluarachchi (2008a) showed that the lumped regionalization method can successfully predict the parameter space of the basin. Additional monitoring and data collection can further improve the calibration results by reducing the uncertainty of this hydrologic model making it more accurate and reliable across all sub-basins. However, the impacts of climate change in the basin on issues such as the environment, water quality, and various socioeconomic attributes need to be investigated to obtain a comprehensive assessment.

References

Block, P. J. 2007. Integrated Management of the Blue Nile Basin in Ethiopia: Hydropower and Irrigation Modeling. Discussion Paper No. 00700, Washington, DC: International Food Policy Research Institute. 25 pp.

Conway, D. 1997. A water balance model of the Upper Blue Nile in Ethiopia. *Hydrological Science Journal* 42(2): 265-286.

Conway, D. 2000. The climate and hydrology of the Upper Blue Nile, Ethiopia. *The Geographical Journal* 166: 49-62.

Conway, D. 2005. From headwater tributaries to international river: Observing and adapting to climate variability and change in the Nile Basin. *Global Environmental Change* 15: 99-114.

Conway, D.; Hulme, M. 1993. Recent fluctuations in precipitation and runoff over the Nile subbasins and their impact on Main Nile discharge. *Climatic Change* 25: 127-151.

Conway, D.; Hulme, M. 1996. The impacts of climate variability and future climate change in the Nile basin on water resources in Egypt. *Water Resources Development* 12(3): 277-296.

Dingman, S. L. 2002. Physical Hydrology. Prentice Hall, Upper Saddle River, NJ, 646 pp.

Drogue, G.; Pfister, L.; Leviandier, T.; El Idrissi, A.; Iffly, J. F.; Matgen, P.; Humbert, J.; Hoffmann, L. 2004. Simulating the spatio-temporal variability of streamflow response to climate change scenarios in a mesoscale basin. *Journal of Hydrology* 293: 255-269.

FAO (Food and Agriculture Organization of the United Nations). 1997. Irrigation potential in Africa: A basin approach. FAO land and water bulletin 4. Available online at *http://www.fao.org/docrep/W4347E/w4347e00.htm* (accessed May, 2007), Rome: FAO Land and Water Development Division, 188 pp.

Frederick, K. D. 2002. Introduction. In: *Water resources and climate change*, Frederick, K. D. (ed.) Northampton MA: Edward Elgar Publishing. 514 pp.

Fowler, H. J.; Kilsby, C. G.; O'Connell, P. E. 2003. Modeling the impacts of climatic change and variability on the reliability, resilience, and vulnerability of a water resource system. *Water Resources Research* 39(8): 1222.

Gamachu, D. 1977. Aspects of climate and water budget in Ethiopia. Addis Ababa, Ethiopia: Addis Ababa University Press. 71 pp.

Gleick, P. H. 1991. The vulnerability of runoff in the Nile basin to climatic changes. *Environmental Professional* 13: 66-73.

Guttman, N. H. 1998. Comparing the Palmer drought severity index and the standardized precipitation Index. *Journal of the American Water Resources Association* 34(1): 113-121.

Hashimoto, T.; Stedinger, J. R.; Loucks, D. P. 1982. Reliability, resiliency, and vulnerability criteria for water resource system performance evaluation. *Water Resources Research* 18: 14-20.

Hayes, M. J.; Svoboda, M.; Wilhite, D. A.; Vanyarkho, O. 1999. Monitoring the 1996 drought using the SPI. *Bulletin of the American Meteorological Society* 80: 429-438.

Hulme, M.; Doherty, R.; Ngara, T.; New, M.; Lister, D. 2001. African climate change: 1900-2100. *Climate Research* 17: 145-168.

IPCC (Intergovernmental Panel on Climate Change). 1999. Guidelines on the use of scenario data for climate impact and adaptation assessment. version 1, prepared by Carter, T. R.; Hulme, M.; Lal, M. Task Group on Scenarios for Climate Impact Assessment. Geneva, Switzerland: IPCC. 69 pp.

IPCC. 2000. Special Report on Emissions Scenarios: A Special Report of Working Group III of the Intergovernmental Panel on Climate Change. Cambridge, UK: Cambridge University Press. 570 pp.

IPCC. 2007. Climate change 2007: Impacts, Adaptation and Vulnerability. Contribution of Working Group II to the Fourth Assessment Report of the Intergovernmental Panel on Climate Change. Cambridge, UK: Cambridge University Press. 976 pp.

Johnson, P. A.; Curtis, P. D. 1994. Water Balance of Blue Nile River Basin in Ethiopia. *Journal of Irrigation and Drainage Engineering* 120(3): 573-560.

Kim, U.; Kaluarachchi, J. J. 2008a. Application of Parameter Estimation and Regionalization Methodologies to Ungauged Basins of the Upper Blue Nile River Basin, Ethiopia. *Journal of Hydrology* (under review).

Kim, U.; Kaluarachchi, J. J. 2008b. Assessment of climate change impacts on water resources of the upper Blue Nile River Basin, Ethiopia. *Water Resources Management* (under review).

Kim, U.; Kaluarachchi, J. J.; Smakhtin, V. U. 2008. Generation of monthly precipitation under climate change for the upper Blue Nile River Basin, Ethiopia. *Journal of American Water Resources Association* (in press).

Kim, U.; Lee, D.; Yoo, C. 2004. Effects of climate change on the streamflow for the Daechung dam watershed. *Journal of Korea Water Resources Association* 37(4): 305-314.

Maier, H. R.; Lence, B. J.; Tolson, B. A.; Foschi, R. O. 2001. First-order reliability method for estimating reliability, vulnerability, and resilience. *Water Resources Research* 37: 779-790.

Martin, G. N. 1973. Characterization of simple exponential baseflow recessions. *Journal of Hydrology New Zealand* 12(1): 57-62.

McKee, T. B.; Doesken, N. J.; Kleist, J. 1993. The relationship of drought frequency and duration to time scales. In: 8th Conference on Applied Climatology, Anaheim, CA, January 17-22, pp 179-184.

MOWR (Ministry of Water Resources). 1998. Abbay River Basin Integrated Development Mater Plan Project: Phase 2, vol. VI, Water Resources Development, part 2, Large Irrigation and Hydropower Dams. Report, Addis Ababa, Ethiopia. pp. 22-24.

Moy, W. S.; Cohon, J. L.; ReVelle, C. S. 1986. A programming model for analysis of the reliability, resilience, and vulnerability of a water supply reservoir. *Water Resources Research* 22(4): 489–498.

Nash, J. E.; Sutcliffe, J. V. 1970. River forecasting using conceptual models: Part 1-A discussion of principles. *Journal of Hydrology* 10: 282-290.

NMSA (National Meteorological Service Agency). 2001. Initial national communication of Ethiopia to the United Nations Framework Convention on Climate Change (UNFCCC). Report, Addis Ababa, Ethiopia, 113 pp.

Palmer, W. C.; Havens, A. V. 1958. A graphical technique for determining evapotranspiration by the Thornthwaite method. *Monthly Weather Review* 86: 123-128.

Seleshi, Y.; Zanke, U. 2004. Recent changes in rainfall and rainy days in Ethiopia. *International Journal of Climatology* 24: 973-983.

Sene, K. J.; Tate, E. L.; Farquharson, F. A. K. 2001. Sensitivity studies of the impacts of climate change on White Nile flows. *Climatic Change* 50: 177-208.

Smakhtin, V. U. 2001. Low flow hydrology: a review. *Journal of Hydrology* 240: 147-186.

Strzepek, K. M.; Yates, D. N. 1996. Economic and social adaptation to climate change impacts on water resources: a case study of Egypt. *Water Resources Development* 12: 229-244.

Sutcliffe, J. V.; Parks, Y. P. 1999. The Hydrology of the Nile. IAHS Special Publication No. 5, IAHS Press, International Association of Hydrological Sciences, Wallingford, England, 179 pp.

Tafesse, T. 2001. The Nile Question: Hydropolitics, Legal Wrangling, Modus Vivendi and perspectives. LIT Verlag, London, 154 pp.

USBR (US Bureau of Reclamation). 1964. Land and Water Resources of the Blue Nile Basin. Main Report, United States Department of Interior Bureau of Reclamation, Washington, DC.

UNESCO (United Nations Educational, Scientific and Cultural Organization). 2004. National Water Development Report for Ethiopia. UN-WATER/WWAP/2006/7, World Water Assessment Program, Report, MOWR, Addis Ababa, Ethiopia, 273 pp.

Vogel, R. M.; Fennessey, N. M. 1994. Flow-duration curves. I: New interpretation and confidence intervals. *Journal of Water Resources Planning and Management* 120(4): 485-504.

WAPCOS (Water and Power Consultancy Services). 1990. Preliminary Water Resources Development Master Plan for Ethiopia. vol. VII, Annex J: Hydropower, Ethiopia Valleys Development studies Authority, Report, Addis Ababa, Ethiopia.

Waterbury, J. 1979. Hydropolitics of the Nile Valley. Syracuse University Press, New York, 301 pp.

Watson, D. F. 1992. Contouring: A guide to the analysis and display of spatial data. Pergamon Press, Oxford, UK, 321 pp.

Whittington, D.; Wu, X.; Sadoff, C. 2005. Water resources management in the Nile basin: the economic value of cooperation. *Water Policy* 7: 227-252.

Wilby, R. L.; Harris, I. 2006. A framework for assessing uncertainties in climate change impacts: Low-flow scenarios for the River Thames, UK. *Water Resources Research* 42: W02419.

Wurbs, R. A.; Muttiah, R. S.; Felden, F. 2005. Incorporation of climate change in water availability modeling. *Journal of Hydrologic Engineering* 10(5): 375-385.

Xu, C. Y. 2000. Modelling the effects of climate change on water resources in central Sweden. *Water Resources Management* 14: 177-189.

Yates, D. N.; Strzepek, K. M. 1996. Modeling economy-wide climate change impacts on Egypt: A case for an integrated approach. *Environmental Modeling and Assessment* 1: 119-135.

Yates, D. N.; Strzepek, K. M. 1998a. An assessment of integrated climate change impacts on the agricultural economy of Egypt. *Climatic Change* 38: 261–287.

Yates, D. N.; Strzepek, K. M. 1998b. Modeling the Nile Basin under climatic change. *Journal of Hydrologic Engineering* 3(2): 98-108.

Zongxue, X.; Jinno, K.; Kawamura, A.; Takesaki, S.; Ito, K. 1998. Performance risk analysis for Fukuoka water-supply system. *Water Resources Management* 12(1): 13–30.

Research Reports

114. *Developing Procedures for Assessment of Ecological Status of Indian River Basins in the Context of Environmental Water Requirements.* Vladimir Smakhtin, Muthukumarasamy Arunachalam, Sandeep Behera, Archana Chatterjee, Srabani Das, Parikshit Gautam, Gaurav D. Joshi, Kumbakonam G. Sivaramakrishnan and K. Sankaran Unni. 2007.

115. *Rural-Urban Food, Nutrient and Virtual Water Flows in Selected West African Cities.* Pay Drechsel, Sophie Graefe and Michael Fink. 2007.

116. *Agricultural Water Management in a Water Stressed Catchment: Lessons from the RIPARWIN Project.* Matthew P. McCartney, Bruce A. Lankford and Henry Mahoo. 2007.

117. *Treadle Pump Irrigation and Poverty in Ghana.* Adetola Adeoti, Boubacar Barry, Regassa Namara, Abdul Kamara and Atsu Titiati. 2007.

118. *Evaluation of Historic, Current and Future Water Demand in the Olifants River Catchment, South Africa.* Matthew McCartney and Roberto Arranz. 2007.

119. *Changing Consumption Patterns: Implications on Food and Water Demand in India.* Upali A. Amarasinghe, Tushaar Shah and Om Prakash Singh. 2007.

120. *Hydrological and Environmental Issues of Interbasin Water Transfers in India: A Case of the Krishna River Basin.* Vladimir Smakhtin, Nilantha Gamage and Luna Bharati. 2007.

121. *Shifting Waterscapes: Explaining Basin Closure in the Lower Krishna Basin, South India.* Jean-Philippe Venot, Hugh Turral, Madar Samad and François Molle. 2007.

122. *Trees and Water: Smallholder Agroforestry on Irrigated Lands in Northern India.* Robert J. Zomer, Deborah A. Bossio, Antonio Trabucco, Li Yuanjie, D. C. Gupta and V. P. Singh. 2007.

123. *India's Water Future to 2025–2050: Business-as-Usual Scenario and Deviations.* Upali A. Amarasinghe, Tushaar Shah, Hugh Turral and B. K. Anand. 2007.

124. *Institutions, Impact Synergies and Food Security: A Methodology with Results from the Kala Oya Basin, Sri Lanka.* Rathinasamy Maria Saleth, Ariel Dinar, Susanne Neubert, Bandi Kamaiah, Seenithamby Manoharan, Sarath Abayawardana, Ranjith Ariyaratne and Shyamalie de Silva. 2007.

125. *The Lower Krishna Basin Trajectory: Relationships between Basin Development and Downstream Environmental Degradation.* Jean-Philippe Venot, Bharat R. Sharma and Kamineni V. G. K. Rao. 2008.

126. *Climate Change Impacts on Hydrology and Water Resources of the Upper Blue Nile River Basin, Ethiopia.* Ungtae Kim, Jagath J. Kaluarachchi and Vladimir U. Smakhtin. 2008.

Postal Address
P O Box 2075
Colombo
Sri Lanka

Location
127, Sunil Mawatha
Pelawatta
Battaramulla
Sri Lanka

Telephone
+94-11-2880000

Fax
+94-11-2786854

E-mail
iwmi@cgiar.org

Website
http://www.iwmi.org

IWMI is a Future Harvest Center
supported by the CGIAR

ISSN: 1026-0862
ISBN: 978-92-9090-696-4